Including thermal network operation in the optimization of a Multi Energy System

Energy Conversion and Management 277 (2023) 116682

Contents lists available at ScienceDirect

Energy Conversion and Management

journal homepage: www.elsevier.com/locate/enconman

Including thermal network operation in the optimization of a Multi Energy System

Umberto Tesio *, Elisa Guelpa, Vittorio Verda

Energy Department of Politecnico di Torino, Turin, Italy

ARTICLE INFO

Keywords:
Decomposed problem
MILP
Near-optimal solution
Iterative process
Thermal storage

ABSTRACT

The combined production of different energy vectors with Multi Energy Systems is a very attractive opportunity to increase the generation efficiency, compensate the oscillations of renewable sources, and improve the flexibility in power generation. Optimizing their operation is a complex task, since the problem can easily reach high dimensions, representing a challenge for commercial solvers. The inclusion in the optimization of a thermal network whose simulation is based on temperatures and flowrates allows to significantly improve the applicability of the obtained results. In addition, the effect of the operating temperatures on the performances of thermal components should be included as well. With these purposes, the present study proposes a strategy for the operation optimization of a MES and its internal thermal network. The model relies on a decomposition approach, where the original problem is divided in two subproblems. In the first one, the MES operating costs are minimized without considering the effects of the thermal network, while in the second one, the thermal network operation is optimized in order to find the operating conditions that are more favourable to the ones found for the MES. These subproblems are iteratively solved until the process converges to a stable solution. Some efforts are taken to keep the mathematical formulation as simple as possible (the MES is a Mixed Integer Linear Programming, while the heating network is a Quadratically Constrained Programming). The developed model allows to find near-optimal solutions which satisfy the numerous physical and technical constraints addressed. The results provide an optimized schedule for the thermal storage in terms of mass flowrates and temperature. One of the strengths of the model is the relatively low computational time required to reach the convergence and, despite not being the global optimum, the high quality of the solution obtained.

1. Introduction

The research in the energy field has been remarkably boosted during the last decades by the goal of reducing the climate changes by keeping the increase of the global average temperature below 1.5 °C ([1]). The production and consumption of energy has been put in discussion, looking in a different perspective the topics of energy efficiency ([2]), ambient pollution, availability of energy sources ([3]), and global warming. Developing new technologies, improving the conversion processes, operating with multiple energy vectors, exploiting energy storages, and increasing the production from renewable sources are some of the main actions recognised to tackle the agreements signed by the international community ([4]). However, executing at the same time these measures to build the next generation of the power production system is still a very complex task, both in theory and in practice ([5]).

In this framework, the Multi Energy Systems (MES) constitute a complete synthesis of these purposes, allowing to perform a combined production of multiple energy vectors using a great variety of sources and technologies ([6]). To set the operation of an energy system it is therefore necessary to establish which technologies will be employed for the combined generation of the energy vectors and the variation of their partial loads during the time interval considered. In the present work, this task will be referred as the "operation optimization of the MES". Among the most important issues that the MES have to face during its operation, there are: i) handling the fluctuations in the power production from renewable sources ([7]); ii) managing the energy storages ([8]); iii) dealing with the mutual dependence and influence on the operation of different components. Considering these requirements, it appears as unavoidable that in order to solve the operation problem, an optimization process must be addressed. Deterministic solvers are the most employed alternative since this kind of problems can easily reach very high dimensions ([9]). In order to represent the MES as accurately as possible, many different real phenomena must be included in the

* Corresponding author.
E-mail addresses: umberto.tesio@polito.it (U. Tesio), elisa.guelpa@polito.it (E. Guelpa), vittorio.verda@polito.it (V. Verda).

https://doi.org/10.1016/j.enconman.2023.116682
Received 8 November 2022; Received in revised form 9 January 2023; Accepted 10 January 2023
Available online 14 January 2023

Nomenclature

a	Coefficient in performance curve
b	Coefficient in performance curve
c	Coefficient in performance curve
c	Specific cost
$\mathscr{C}$	Set of components
c_p	Specific heat
d	Coefficient in performance curve
e	Coefficient in performance curve
E	Energy
h	Binary variable for piecewise linearization
k	Start-up/shut-down state of components
l	Storage loss coefficient
$\dot{m}$	Mass flowrate
M	Mass
$\mathscr{M}$	Big-M
P	Power
s	Operating state of components
t	Time
T	Temperature
$\mathscr{T}$	Set of timesteps
$\mathscr{V}$	Set of energy vectors
w	Weight parameter
x	Constant value for piecewise linearization
y	Constant value for piecewise linearization
z	Constant value for piecewise linearization

Abbreviations

CFVT	Constant flow and variable temperature
CHP	Combined heat and power system
DHN	District heating network
EHP	Electric heat pump
FC	Fuel cell
GHP	Gas heat pump
HOB	Heat only boiler
LP	Linear Programming
LPG	Liquefied petroleum gas
MES	Multi energy system
MILP	Mixed integer linear programming
MINLP	Mixed integer nonlinear programming
NG	Natural gas
NLP	Nonlinear programming
OF	Objective function
PV	Photovoltaic
QCP	Quadratically constrained programming
SoC	State of charge
TN	Thermal network
VFCT	Variable flow and constant temperature
VFVT	Variable flow and variable temperature

Greek letters

α	Continuous variable for piecewise linearization
β	Binary variable for storage
Δ	Difference
ϵ	Absolute error
Ψ	Convergence parameter
Φ	Heat flux

Superscripts

ch	Charging
dis	Discharging
k	Index for iterations
l	Lower
max	Maximum
min	Minimum
t	Index for timesteps
th	Thermal
u	Upper

Subscripts

amb	Ambient
ave	Average
buy	Energy bought
C	Cold
cmp	Component
f	Index for fuels
H	Hot
i	Generic index
in	Inlet
j	Generic index
off	Off
on	On
out	Outlet
sell	Energy sold
stor	Storage
t	Index for timesteps
w	Water

model. As a consequence, many nonlinear and nonconvex terms are likely to appear in the model. In this way, the complexity of the problem increases significantly and the capability of finding the global optimum as outcome of the optimization is compromised. For these reasons, it is preferred to develop a model with a linear formulation, such that Mixed Integer Linear Programming (MILP) solvers with an advanced stage of development can be exploited ([10]). Noticeable efforts are therefore made in converting Mixed Integer Nonlinear Programming (MINLP) models into MILPs (or at least into convex MINLPs). The most employed strategies for this task are ([11]): i) linearization of nonlinearities ([12]); convexification of nonconvex terms ([13]); problem decomposition. Nonlinearities are treated according to their nature; the addition of auxiliary variables is always needed, which can be both continuous and binary ([14]). Convexification strategies are employed to reduce the complexity of the optimization problem and obtain global optimums instead of local optimums. Since they usually rely on relaxation techniques, iterative processes are often needed to tighten the approximation and increase the feasibility of the solution ([15]). Finally, the problem decomposition aims at separating the complete problem into smaller (and simpler) ones, which can be solved quickly. The separation can be either conceptual, when the subproblems represent portions of the system ([16]), or mathematical, when the subproblems are divided according to their mathematical formulation ([17]). The benefits brought by these approaches increase while increasing the complexity of the problem under consideration.

Any kind of technology for the energy production can be included in a MES, and the most considered ones are: combined heat and power, heat only boilers, electric heat pumps, fuel cells, photovoltaic panels, and wind turbines. Other peculiar elements are energy storages and the connections with the external grids. In addition, the exchange of both electrical and thermal powers is performed by means of energy networks ([18]), which are very important infrastructures and whose operation must be carefully assessed ([19]). However, including their simulation in the MES operation optimization results to be very challenging, because of the very high number of additional variables that should be introduced and the mathematical form of the constraints that must be

addressed to simulate the physical behaviour of the networks. In particular, including the Thermal Network (TN) in the optimization would guarantee the feasibility of the solution in the real application. Another advantage brought by this combined optimization is represented by the possibility to increase the flexibility of the system, allowing to obtain higher-quality solutions. However, because of the challenges already mentioned, most of the studies that in the scientific literature do not implement the simulation of the thermal network in the model created for the MES operation optimization. For example, detailed and reliable optimizations are developed for MESs subserved to a hospital ([20]), a tile factory ([21]), and generic loads ([22]), but in none of them is simulated the thermal network. On a physical perspective it represents an acceptable simplification since the consistency of the problem is granted by simply addressing the energy balance between the thermal powers consumed and generated, despite the accuracy of the simulation will be unavoidably reduced.

Some available works include the thermal network in the optimization in very different ways. In few cases it is implemented by computing the heat powers transferred between the nodes ([23,24]). This basic approach is mostly adopted when the design of the TN is one of the aspects that must be optimized. In fact, knowing the amount of heat exchanged between two nodes, it is possible to estimate the size and cost of the pipe that must be installed. However, this strategy does not allow to address the problem of the TN operation. When a higher degree of precision is required for the operation of the thermal network, it becomes necessary to consider the operating mass flowrates and temperatures, beside addressing some initial hypothesis. In addition, different control strategies can be chosen. The Constant Flow and Variable Temperature (CFVT or quality regulation) is a common choice in the research since it is the most employed strategy in the real world. This control strategy is adopted in [25] and [26], where the building inertia is included to increase the flexibility of the system. The main transport networks are implemented in [27], where CFVT is used for the DH management and the optimization results are compared with traditional control strategies, showing advantages both in economic and environmental terms. The opposite alternative is the Variable Flow and Constant Temperature (VFCT or quantity regulation) strategy, which is less investigated. This option is chosen in [28] to optimize the design and operation of a system in the perspective of distributed energy resources. These two strategies allows to keep a linear formulation of the TN, since only one between the mass flowrates and temperatures must be considered as independent variable. This linearity is lost with the Variable Flow and Variable Temperature (VFVT) strategy, characterized by a higher degree of freedom that can be achieved in the regulation. This strategy allows to reach a higher number of operating conditions, which can result to be more advantageous for the thermal production with respect to the ones reached with the CFVT or VFCT. However, for this same reason, the VFVT is also the most complex to implement in the optimization, due to its nonconvex mathematical formulation. In particular, because of the product between mass flowrates and temperatures (bilinear terms), the energy balances at the nodes of the network are nonlinear and nonconvex equations. Taking into account the quantity and the nature of these bilinear terms, using a piecewise linearization technique on the energy balances results to be unfeasible. In fact, the problem sizes would increase dramatically, and the collateral high number of binary variables would compromise the problem convergence in an acceptable computational time. On the other hand, keeping the nonconvex Mixed Integer Quadratically Constrained program (MIQCP) formulation make necessary to execute the optimization with a suitable solver (i.e. Gurobi [29] or Ipopt [30]). Relaxation techniques (e.g. Mc Cormick relaxation) are used by the solvers, with the help of complex iterative strategies (spatial branches, cutting planes, etc.) implemented to improve the relaxation and guarantee the feasibility of the solution. However, the MIQCP sizes that can be handled by commercial solvers are still too small compared to the typical ones of a MES problem. The last option for handling these constraints can rely on a decomposition approach. The concept behind this strategy relies on the idea that a series of small problems can be solved faster than a single problem with dimensions equal to the sum of the smaller ones. Incremental piecewise linearization and relaxation of bilinear terms are used in [31], where the convergence to a feasible solution is managed with a parallel Benders decomposition combined with the sequential bound-tightening. Finally, the simulation of a MES including electrical and thermal networks is performed in [32] with two strategies: a sequential approach, where the electrical, hydraulic and thermal problems are solved in series; and an integrated approach, where the problems are managed in parallel.

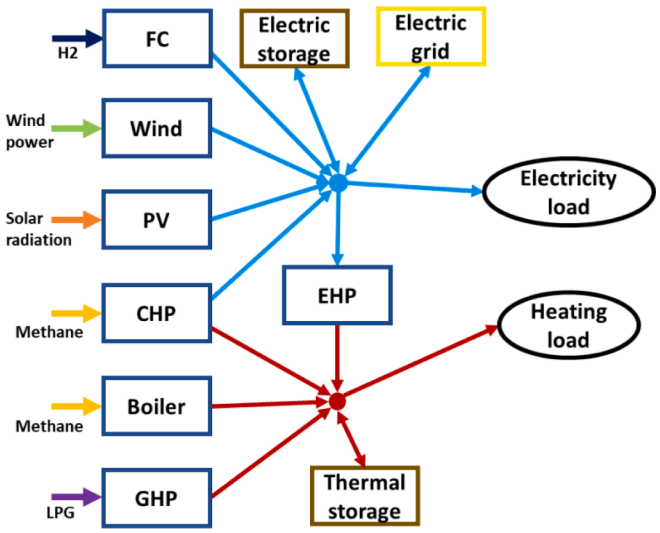

Fig. 1. Simplified schematic of the MES analysed.

The aim of the present study is to investigate the inclusion of the thermal network simulation (with the VFVT strategy) in the operation optimization of a MES. A relatively basic case study is chosen, characterized by a thermal network of small dimensions. The performances of the technologies are addressed such that the dependence on both the partial load and the operating temperatures are considered, which is one of the novelties of the present work. Taking advantage of this characteristic, an original strategy for solving efficiently the combined operation of the energy system and the thermal network has been developed. Another important novelty of the present study is represented by the implementation of a thermal storage in the thermal network, whose simulation takes into account the temperature of the water stored. The model relies on linearization and decomposition techniques, and, in authors' knowledge, its main structure has never been investigated before. The iterative process developed to solve the decomposed problem does not ensure the achievement of the global optimum and must be therefore considered as a near-optimum solution. However, the quality of the optimization outcome is demonstrated to be adequate, especially considering the non-demanding computational times requested by the process to solve the operation problem.

2. Case study

The MES considered in the present work has a relatively simple structure, which is shown in Fig. 1. All the energy vectors and technologies involved in the MES operation are reported in this image. The energy system has the task of satisfying the demand of two energy vectors: electricity (in light blue) and heating (in red). Concerning the fuels, methane (in yellow), hydrogen (in blue) and LPG (in purple) are considered in the present work. The production process of the hydrogen is not included in the analysis, therefore it is assumed as a fuel imported from the outside of the system. It is worth to mention that connections represented for the exchange of the thermal powers must be considered

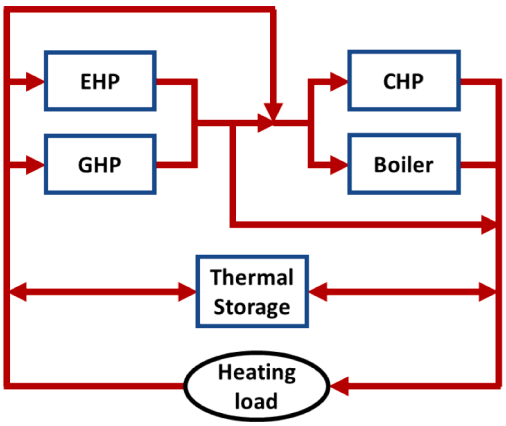

Fig. 2. Layout of the heating network of the MES.

only as conceptual and not as topological (i.e. the real layout of the networks is different from the one represented in the figure).

The technologies involved in the electricity/heating generation are: Combined Heat and Power (CHP), Heat only Boiler (HOB), Electric Heat Pump (EHP), Gas Heat Pump (GHP), Fuel Cell (FC), Photovoltaic panels (PV), wind turbine (Wind), electric storage, thermal storage and the connection with the electric grid. Any other technology can be included, since, as exposed in the next section, the mathematical formulation used to model the components does not change with their typology.

As time period, a single day (24 h) discretized with a timestep of 15 min is considered for the present study.

Being out of the extents of this analysis, the electric grid is not simulated and only its connection with the MES is considered.

In order to model the heat transportation, it is necessary to point out the important distinction between thermal networks inside the MESs and external District Heating Networks (DHNs). The latter ones are usually characterized by medium/large size, which can be between a small city up to an entire town. The DHNs topology can be either ring-shaped or tree-shaped, and it is constituted by two pipes (for the supply and the return of the hot water). In addition, the noticeable spatial extension of DHNs determines non-negligible heat dispersions (due to convection heat losses) and time delays in the propagation of hot water across the pipes.

On the other side, thermal networks operating inside MESs are required to connect the technologies producing or consuming heat. In this kind of systems, these components are located relatively close. As a result, the effects determined by the thermal inertia of the network and the heat losses can be neglected, introducing a reasonable simplifying hypothesis, adopted in this analysis. In addition, the layout of MESs networks can present many differences compared to DHNs. For example, the distinction between supply and return pipes may not be straightforward as in the case of DH, since more complex connections could link the technologies. Each thermal generator is equipped with a water pump and the mass flows circulating in the network can be adjusted more precisely with respect to DHNs, where, in case of meshes, it is not always possible to impose all the flowrates. In light of that, the present study is conducted assuming that all the directions of the mass flowrates are known, and any amount of flowrate can be set in each branch. In addition, from now on, the thermal infrastructure for the exchange of heating powers considered in this case study will be synthetically referred as TN, remembering that it is only a thermal network inside the MES and not an external DHN. Beside the internal TN of the MES, no other DHNs are considered and simulated in the present analysis.

The layout of the thermal network taken as case study in the present work is shown in Fig. 2. This setting is selected since it provides a high degree of freedom for the operation of the network itself. The thermal generators are coupled such that the EHP and the GHP are connected in parallel, and the same is done for the boiler and the CHP. Each of the two couples has a bypass branch that allows to skip the components whenever they are not operating, or it is needed to meet technical constraints on temperatures/flowrates across the network. Each component can operate independently from the other it is coupled to, and either the separate or simultaneous operation of the two couples is possible. In this last case, the two couples can be connected both in parallel and in series. In case of series connection, the couple composed by the two heat pumps is placed for first because the outlet temperatures attained by these technologies are typically lower than the ones reached by HoBs and CHPs.

Finally, it is worth to mention that, despite the case study analysed in the present work has been freely developed by authors and it is not referred to any specific sector, the real applications for these kind of energy systems are particularly wide. Centralized power production, heavy industries, energy communities, distributed generation, near zero energy buildings and some tertiary industries (e.g. hospitals) are the main examples of real contexts in which energy systems can operate.

3. Methodology

The aim of this work is to develop a model for optimizing the operation of a Multi Energy System, including the operation of the thermal network. As thermal network is intended the system that allows the heat transportation among the thermal generators and the thermal load. The VFVT regulation of the network makes possible to achieve the highest degree of freedom in the operation and it is reasonable to expect that the energy system will take advantage from that (in fact, this is the regulation adopted for the thermal network).

This section is devoted to the explanation of the model developed in the present work. The approaches adopted to represent the operation of the generators and the physical behaviour of the thermal network are discussed in two separate paragraphs.

3.1. Modelling of components

In this paragraph the formulations exploited in the model in order to represent the operation of the elements constituting the MES in a mathematical form are described. For first, the approach to model the technology performance is discussed. Then, the constraints representing the technical boundaries for their operation are addressed.

3.1.1. Performances of components

The performances of the technologies constituting the MESs are widely recognised by the scientific literature to be nonlinear ([10]). The most common formulation to represent the operation of the components is a third-degree polynomial with a single variable. Typically, the independent variable is the input power (the power of the fuel/vector consumed), while the dependent variable is the output power (the power of the energy vector produced). In addition, a more detailed description can be achieved by using a polynomial with two independent variables, which may be preferred in case of components with a relatively complex operation, such as the CHP ([22]).

One of the aims of the present study is to include the effects of the operating temperature of the thermal generators on their performance. With this purpose, a parameter that will be called “characteristic temperature” is defined for each heat generator. The characteristic temperature can be defined as the temperature that is able to represent the dependence of the efficiency on the operating temperatures; this can be, depending on the technology, the temperature at the inlet, at the outlet, the average between these two, or any other form. As a consequence, two independent variables are addressed to describe the performance of the technologies adopted: the inlet power (P_{in}), and the characteristic temperature (T_{cmp}). This can be seen in the general formulation of the performance of the components, reported in Equation (1), where P_{out} is the outlet power, while a, b, c, d, and e are fixed numerical coefficients. As arbitrary choice, the T_{cmp} appears only at first-degree in the

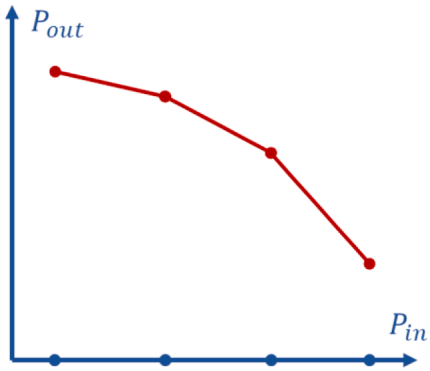

Fig. 3. Conceptual representation of a 1-D piecewise linearization.

polynomial; however, because to the approach adopted to implement the optimization, any other degree can be chosen in the equation.

$$P_{out} = a \cdot P_{in}^3 + b \cdot P_{in}^2 + c \cdot P_{in} + d \cdot T_{cmp} + e \quad (1)$$

Concerning the optimization process, developing a model with a linear formulation would guarantee the achievement of the global optimum and would allow to use commercial solvers with an advanced stage of development. This advantage is the reason because a noticeable number of papers exist in the scientific literature in which a LP or MILP formulation is chosen. For this reason, Equation (1) is linearized with the piecewise approach. A description of the linearization strategy is reported in the following subparagraphs, while the detailed explanation of the method adopted is presented in [33].

- 1D linearization

The performance curve is discretized into different segments by fixing some values of the independent variable (x_i) inside of its range of variation, and the corresponding values of the dependent variable (y_i), where the subscript i goes from 1 to the number of linearization nodes N (this set is named $\mathcal{I}$). Then, a continuous variable (α_i, bounded between 0 and 1) is associated to each node, while a binary variable (h_i) is assigned to each segment of linearization. After having added some constraints on these linearization variables (details in [33]), it is possible to reformulate the original variables as shown in Equations (2) and (3):

$$P_{in} = \sum_{i \in \mathcal{I}} [x_i \cdot \alpha_i] \quad (2)$$

$$P_{out} = \sum_{i \in \mathcal{I}} [y_i \cdot \alpha_i] \quad (3)$$

This kind of linearization is visually represented in Fig. 3, where a nonlinear performance curve is linearized in 3 intervals (4 linearization nodes).

- 2D linearization

The 2D linearization is more complex with respect to the 1D linearization. Because of its higher accuracy, the technique adopted in this study relies on the triangle method. The performance surface is discretized with a mesh, fixing some values of the independent variables (x_i, y_j) inside of their domain, and the corresponding values of the dependent variable (z_{ij}). Then, a continuous variable (α_{ij}, bounded between 0 and 1) is associated to each mesh node, while two binary variables (h_{ij}^l and h_{ij}^u) are assigned to each sector of the mesh. Other constraints on these linearization variables are added (details in [33]), then, it is possible to reformulate the original variables as shown in Equations 4–6:

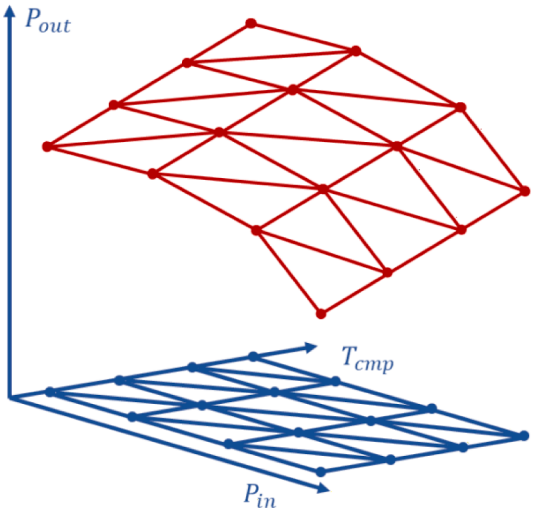

Fig. 4. Conceptual representation of a 2-D piecewise linearization.

Table 1
Parameters taken as characteristic temperatures and linearization intervals.

		CHP	Boiler	GHP	EHP	FC
Independent variables	P_{in}	*	*	*	*	*
	T_{cmp}	*(T_{in})	*(T_{in})	*(T_{out})	*(T_{out})	×
Linearization nodes		4x4	4x4	4x4	4x4	4

$$P_{in} = \sum_{i \in \mathcal{I}} \left[x_i \sum_{j \in \mathcal{J}} [\alpha_{ij}] \right] \quad (4)$$

$$T_{cmp} = \sum_{j \in \mathcal{J}} \left[y_j \sum_{i \in \mathcal{I}} [\alpha_{ij}] \right] \quad (5)$$

$$P_{out} = \sum_{i \in \mathcal{I}, j \in \mathcal{J}} [z_{ij} \cdot \alpha_{ij}] \quad (6)$$

This kind of linearization is visually represented in Fig. 4, where a nonlinear performance surface is linearized in 18 intervals (4x4 linearization nodes).

Finally, the dependencies of the operation of the components and the discretization of their performances are reported in Table 1.

Energy storages require a different modelling with respect to the other technologies. The simplest approach consists in addressing a single continuous variable and the capacity constraints, which are sufficient to simulate the storage operation. However, if more complex constraints are addressed (e.g. layout connections among technologies), a more detailed description is required. For this reason, the energy storage is simulated with two continuous variables (P_{stor}^{ch} for the charging phase and P_{stor}^{dis} for the discharging phase) and one binary variable (β), which avoids a simultaneous charge and discharge of the storage.

3.1.2. Components constraints

The constraints addressed to bound the operation of the components to their technical limitations are reported below.

- Energy vectors balances

This constraint imposes that, for each timestep and for each energy vector, the sum of the powers produced by the generators is equal to the sum of those absorbed by the consumers. Its mathematical formulation is reported in Equation (7), where $\mathcal{C}$, $\mathcal{V}$ and $\mathcal{T}$ are respectively the sets of the components c, energy vectors v and timesteps t.

$$\sum_{c\in\mathscr{C}}\left[P_c^{v,t}\right]=0\forall v\in\mathscr{V};\forall t\in\mathscr{T} \tag{7}$$

- Minimum on/off times

An important characteristic of the technologies involved in the MESs is that their operation in time cannot be excessively discontinuous. A high number of start-ups and shutdowns in a short amount of time can have deleterious effects on their lifecycle, and it may be infeasible in practical terms. For these reasons, the constraints imposing the minimum time interval in which a component cannot change its operating state (after a start-up or a shutdown) are implemented. For first, the operation state (s, 1/0 for on/off) of each component is obtained with Equation (8); then, an auxiliary dependent variable (k) is computed with Equation (9). Finally, the constraint on the minimum operating time after a start-up is imposed by Equations (10) and (11), while the minimum operating time after a shutdown is imposed by Equation (12) and (13). Here, $N_{t,on/off}$ is the number of timesteps in which the component cannot change its operating state after a start-up or a shutdown, while $\mathscr{M}$ is the so called Big-M, a constant number that is fixed to an arbitrary high value.

$$s^t=\sum_{i\in\mathscr{I}}\left[h_i^t\right]or\sum_{i\in\mathscr{I},j\in\mathscr{J}}\left[h_{ij}^{l,t}+h_{ij}^{u,t}\right] \tag{8}$$

$$k^t=s^t-s^{t-1} \tag{9}$$

$$\sum_{t=t^*}^{t^*+N_{t,on}-1}\left[s^t\right]-N_{t,on}\le\left(1-k^{t^*}\right)\cdot\mathscr{M} \tag{10}$$

$$\left(k^{t^*}-1\right)\cdot\mathscr{M}\le\sum_{t=t^*}^{t^*+N_{t,on}-1}\left[s^t\right]-N_{t,on} \tag{11}$$

$$\sum_{t=t^*}^{t^*+N_{t,off}-1}\left[s^t\right]\le\left(1+k^{t^*}\right)\cdot\mathscr{M} \tag{12}$$

$$-\left(k^{t^*}+1\right)\cdot\mathscr{M}\le\sum_{t=t^*}^{t^*+N_{t,off}-1}\left[s^t\right] \tag{13}$$

- Ramping constraints

Similarly to the constraints on the minimum on/off time, the ramping constraints are addressed to represent the dynamics of the components. In particular, their implementation avoid that their operation undergoes too extended changes in short amounts of time. The ramp-up and ramp-down constraints are typically referred to the operating power. However, in order to represent the inertia of the components in changing their operating temperatures, the ramping constraints are implemented for the T_{cmp} (Equation (14)). Here, $\mathscr{C}^{th}$ is the set of components whose performance depend on T_{cmp}, while $\Delta T_{cmp}^{max/min}$ is the maximum/minimum difference of characteristic temperature that must be respected.

$$\Delta T_{cmp,c}^{min}-\mathscr{M}\cdot\left(2-s_c^t-s_c^{t-1}\right)\le T_{cmp,c}^t-T_{cmp,c}^{t-1}\le\Delta T_{cmp,c}^{max}+\mathscr{M}\cdot\left(2-s_c^t-s_c^{t-1}\right)\quad\forall c\in\mathscr{C}^{th} \tag{14}$$

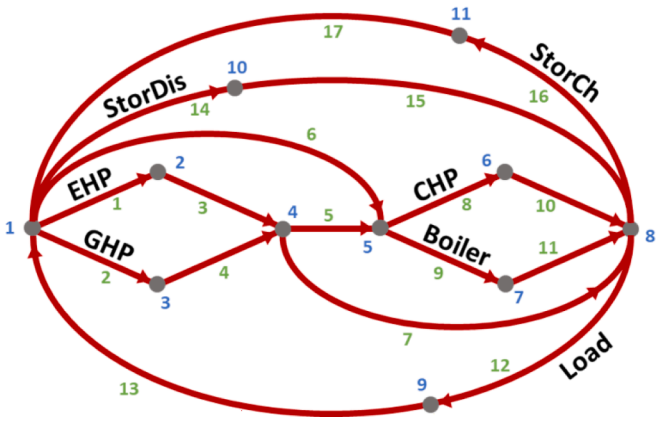

Fig. 5. Graph representation of the thermal network.

- Energy storage

As already discussed, each energy storage is modelled with two continuous variables, one binary variable and some devoted constraints. The State of Charge (SoC) is computed with Equation (15), where the energy losses (l^{stor}) are included and modelled as a fraction of the SoC itself. The maximum and minimum storage capacity achievable during the operation are imposed with Equation (16), while Equations (17) and (18) are addressed in order to avoid the simultaneous charging and discharging of the component. Notice that when an energy storage is simulated only with the charging/discharging power and its state of charge, the mathematical formulation does not change if either an electrical or thermal storage is considered.

$$SoC_c^t=\left(1-l_c^{stor}\right)\cdot SoC_c^{t-1}+\left(P_{ch,c}^{v,t}-P_{dis,c}^{v,t}\right)\cdot\Delta t\quad\forall c\in\mathscr{C}^{stor};\ \forall v\in\mathscr{V}^{stor};\ \forall t\in\mathscr{T} \tag{15}$$

$$SoC_c^{min}\le SoC_c^t\le SoC_c^{max}\quad\forall c\in\mathscr{C}^{stor};\quad\forall t\in\mathscr{T} \tag{16}$$

$$0\le P_{ch,c}^{v,t}\le P_{ch,c}^{v,max}\cdot\left(1-\beta_c^t\right)\quad\forall c\in\mathscr{C}^{stor};\ \forall v\in\mathscr{V}^{stor};\ \forall t\in\mathscr{T} \tag{17}$$

$$0\le P_{dis,c}^{v,t}\le\beta_c^t\cdot P_{dis,c}^{v,max}\quad\forall c\in\mathscr{C}^{stor};\ \forall v\in\mathscr{V}^{stor};\ \forall t\in\mathscr{T} \tag{18}$$

3.2. Modelling of thermal network

In order to include the thermal network in the MES operation optimization, it is necessary to build a model that simulates the network operation according to the input data and assumptions adopted for the present analysis. Since the VFVT is the control strategy adopted to manage the network operation, the thermal power transferred are not sufficient to model the grid. Both the mass flowrates ($\dot{m}$) and the temperatures (T) must be assumed as parameters describing the network. With this purpose, the TN layout is designed with the graph approach, as shown in Fig. 5. The branches representing the thermal generators/consumers are labelled with their corresponding name/acronym, while the others are simple pipes connecting the nodes.

On a theoretical level, with the graph approach, each component involved in the thermal generation/consumption could be modelled with a single branch and the corresponding heating flux provided/absorbed. However, according to the TN layout, with this approach it

may happen that the water temperature at the outlet of a component and the temperature of the exit node of the branch are not the same. In particular, this would happen when then the outlet flow of a thermal unit is mixed with another flowrate. For this reason, the thermal units are modelled with two branches in series, such that the identification of the outlet temperature of the components is immediate.

A different approach is developed to simulate the thermal storage, which is modelled with four branches: two for the discharging phases and other two for the charging phases. The reason for this choice relies in the fact that the directions of the flowrates circulating in the network must be fixed a priori. This cannot be done without addressing the simulation of the charging and discharging processes in different branches, since the direction of their water flows is opposite.

The resulting graph of the thermal network is relatively small, since it is composed by 11 nodes and 17 branches. For this reason, it is considered a good starting point for the execution of the innovative method developed in this study. The model of the thermal network is synthesized according to the simplifying assumptions adopted. In fact, since thermal losses and inertia are neglected, each timestep can be assumed to operate in steady-state conditions. For the purpose of the optimization, once that the independent variables are defined, the TN is modelled by addressing the constraints.

3.2.1. Thermal network constraints

This paragraph is devoted to the presentation and discussion of the constraints addressed in order to model the thermal network.

- **Mass flowrate balance**

The mass conservation is imposed implementing one balance equation at each node. Since the network does not present external injections/extractions of water, the sum of the flowrates circulating in the inlet branches must be equal to the sum of the flowrates circulating in the outlet branches. This concept is written in mathematical form in Equation (19), where $\mathcal{N}$ is the set of all the nodes of the network, while IN^k and OUT^k are the sets composed by the upstream and downstream branches of node k, respectively.

$$\sum_{i\in IN^k}\left[\dot{m}_i^t\right]=\sum_{j\in OUT^k}\left[\dot{m}_j^t\right] \quad \forall k\in\mathcal{N};\ \forall t\in\mathcal{T} \tag{19}$$

- **Energy balance**

Energy balances are the constraints ensuring the satisfaction of the first thermodynamic principle. The variables involved are: i) the mass flowrates and the temperatures of the upstream flows mixing in a node; ii) the mass flowrates and the temperatures of the downstream flows of the same node; and iii) the heat fluxes exchanged by the upstream branches, representing a heat production/consumption. This constraint is addressed with Equation (20), where $c_{p,w}$ is the specific heat capacity of water and Φ_i is the thermal flux exchanged by the inlet branch i.

$$\sum_{i\in IN^k}\left[c_{p,w}\cdot\dot{m}_i^t\cdot T_i^t+\Phi_i^t\right]=\sum_{j\in OUT^k}\left[c_{p,w}\cdot\dot{m}_j^t\cdot T_j^t\right] \quad \forall k\in\mathcal{N};\ \ \forall t\in\mathcal{T} \tag{20}$$

- **Temperature boundaries of components**

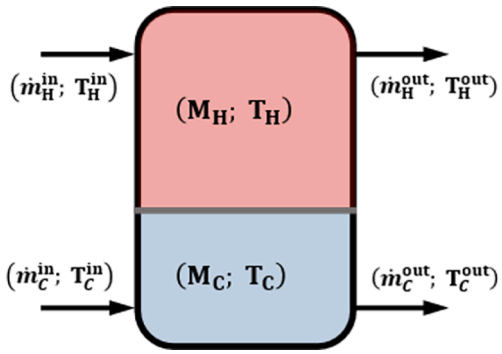

Fig. 6. Schematic of the thermal storage according to the model adopted in the analysis.

and outlet. Since these constraints are needed to be respected only when the component is operating, the big-M technique is again exploited to address them. Their mathematical formulation is reported in Equations (21) and (22).

$$T_{c,min}^{in}-\mathcal{M}\cdot\left(1-s_c^t\right)\le T_c^{in,t}\le T_{c,max}^{in}+\mathcal{M}\cdot\left(1-s_c^t\right) \quad \forall c\in\mathcal{C}^{th};\ \forall t\in\mathcal{T} \tag{21}$$

$$T_{c,min}^{out}-\mathcal{M}\cdot\left(1-s_c^t\right)\le T_c^{out,t}\le T_{c,max}^{out}+\mathcal{M}\cdot\left(1-s_c^t\right) \quad \forall c\in\mathcal{C}^{th};\ \forall t\in\mathcal{T} \tag{22}$$

- **Temperature differences of components**

Beside the boundaries on the inlet/outlet temperature of the components, the operation of the technologies can be limited by constraints on the minimum or maximum temperature difference that the water can undergo by passing through the component itself. These constraints can be easily implemented with the same strategy presented before, as shown by Equation (23).

$$\Delta T_{c,min}-\mathcal{M}\cdot\left(1-s_c^t\right)\le\Delta T_c^t\le\Delta T_{c,max}+\mathcal{M}\cdot\left(1-s_c^t\right) \quad \forall c\in\mathcal{C}^{th};\ \forall t\in\mathcal{T} \tag{23}$$

- **Ramping constraints on T_{cmp}**

In order to be consistent with the MES model, the same ramping constraints on the characteristic temperatures of the components are implemented in the model of the thermal network. Their mathematical formulation is the same reported in Equation (14). However, there is an important difference that is worth to be noticed: the T_{cmp} is not a dependent variable computed with Equation (5), but it is independent, belonging to the set of T defined for the nodes of the thermal network.

- **Ramping constraints on flowrates**

Another kind of ramping constraint should be addressed for the ramp up/down of the mass flowrates crossing the heat generators/consumers. In fact, steep variations of the water flows could be impossible to be executed and, in general terms, it should be preferable to keep relatively continuous operating conditions.

With this purpose, Equation (24) is implemented in the model.

$$\Delta\dot{m}_{c,min}-\mathcal{M}\cdot\left(2-s_c^t-s_c^{t-1}\right)\le\dot{m}_c^t-\dot{m}_c^{t-1}\le\Delta\dot{m}_{c,max}+\mathcal{M}\cdot\left(2-s_c^t-s_c^{t-1}\right) \quad \forall c\in\mathcal{C}^{th};\ \forall t\in\mathcal{T} \tag{24}$$

The different technologies involved in the operation of the thermal network are expected to have a range of temperatures at both their inlet

- **Thermal storage**

The operation of the thermal storage is simulated according to three simplifying assumptions: i) the storage is divided into two water masses, one is hot and the other one is cold; ii) each of these two masses is perfectly mixed (i.e. the temperature is uniform); iii) the two water masses can exchange thermal powers with the external environment, but not between them. Both the hot and cold water masses have an inlet and an outlet stream, as can be seen in the simple schematic reported in Fig. 6. The highlighted parameters are: mass of the cold/hot water ($M_{C/H}$); temperature of the cold/hot water ($T_{C/H}$); inlet/outlet flowrates of cold/hot water ($\dot{m}_{C/H}^{in/out}$); temperature of inlet/outlet flowrates of cold/hot water ($T_{C/H}^{in/out}$).

The operation of the thermal storage is established with the MES optimization, but only in terms of heating powers. A more detailed simulation of the storage operation is obtained addressing Equations 25–31, where the temperatures and mass flowrates of the are taken into account. In particular, Equation (25) is defined for the mass conservation of the hot/cold water; Equation (26) imposes that the hot/cold water mass is between zero and the total mass of the storage (M_{stor}); Equation (27) is implemented for the energy conservation of the hot/cold water; thermal losses are defined in Equation (28); and finally, the temperature of the streams extracted from the storage is defined in Equation (29); and finally, Equation (32) imposes that the energy contained in the storage ($E^{stor,t}$, computed with Equation (34)) is equal to the one found with the MES optimization ($E_{MES}^{stor,t}$).

$$M_{H/C}^{t+1} = M_{H/C}^{t} + \left(\dot{m}_{H/C}^{in,t} - \dot{m}_{H/C}^{out,t}\right)\cdot\Delta t \quad \forall t \in \mathscr{T} \tag{25}$$

$$0 \le M_{H/C}^{t} \le M_{stor} \quad \forall t \in \mathscr{T} \tag{26}$$

$$M_{H/C}^{t+1}\cdot T_{H/C}^{t+1} = M_{H/C}^{t}\cdot T_{H/C}^{t} + \left(\dot{m}_{H/C}^{in,t}\cdot T_{H/C}^{in,t} - \dot{m}_{H/C}^{out,t}\cdot T_{H/C}^{out,t} + \frac{\Phi_{H/C}^{loss,t}}{c_{p,w}}\right)\cdot\Delta t \quad \forall t \in \mathscr{T} \tag{27}$$

$$\left|\Phi_{H/C}^{loss,t}\right| = \frac{I^{stor}\cdot M_{H/C}^{t}\cdot c_p\cdot\left(T_{H/C}^{t} - T_{amb}\right)}{\Delta t} \quad \forall t \in \mathscr{T} \tag{28}$$

$$T_{H/C}^{out,t} = T_{H/C}^{t} + \frac{\Delta t\cdot\Phi_{H/C}^{loss,t}}{c_p\cdot M_{H/C}^{t}} = T_{H/C}^{t} - \left(T_{H/C}^{t} - T_{amb}\right)\cdot l^{stor} \quad \forall t \in \mathscr{T} \tag{29}$$

$$E^{stor,t} = E_{MES}^{stor,t} \quad \forall t \in \mathscr{T} \tag{30}$$

$$E^{stor,t} = c_{p,w}\cdot\left(M_H^{t}\cdot T_H^{t} + M_C^{t}\cdot T_C^{t}\right) \; \forall t \in \mathscr{T} \tag{31}$$

As can be observed in Equation (25), the mass of the hot/cold water can be computed with a linear equation from the corresponding flowrates in the thermal network. However, this does not happen for their temperature, and indeed, the only way to compute them consists in solving a nonlinear equation with independent variables at the denominator of a fraction. This kind of nonlinearity is relatively complex to be managed and most of the commercial solvers does not support its implementation. For this reason, the $T_{H/C}$ are introduced as independent variables to be optimized, such that the mathematical formulation of the energy balances for the thermal storage is quadratic.

3.3. Objective function

According to the criterion that is intended to pursuit (minimization of primary energy consumption, economic costs, CO_2 emissions), different objective functions can be chosen. For the present study, the economic objective function is selected. As a consequence, minimizing the expenditures to sustain during the system operation is the scope of the optimization. This function (Equation (32)) is defined as the summation of the operating costs determined by the purchase of fuels, the maintenance costs (which are collateral to the components operation), and the costs/earnings due to the purchase/sell of electricity from/to the grid. Regarding the mathematical notation, the subscript f is the index for the fuels belonging to the set $\mathscr{F}$; c is the specific cost of fuels/energy vectors; c^m is the specific maintenance cost; and $P_{buy/sell}$ is the power bought/sold to the external grid.

$$OF = \sum_{t\in\mathscr{T}}\left[\sum_{f\in\mathscr{F}}\left[c_f\cdot P_f^{t}\right] + \sum_{c\in\mathscr{C}}\left[c_c^{m}\cdot s_c^{t}\cdot\Delta t\right] + c_{buy}^{el}\cdot P_{buy}^{el,t} - c_{sell}^{el}\cdot P_{sell}^{el,t}\right] \tag{32}$$

Table 2
Variables and constraints of the complete problem.

	MES	TN	Total
Binary variables	7392	0	7392
Continuous variables	7104	2882	9986
Linear equalities	770	1248	18,456
Linear inequalities	10,936	5502	
Quadratic equalities	0	1344	1344

3.4. Decomposition approach for near-optimal solution

The complete model of the system considered as case study is composed by the union of the two sub-models described in the previous paragraphs: the MES model and the model of the thermal network. The size of the problem is determined by the number of components, the level of detail chosen for the piecewise linearization, and the number of timesteps considered. The layout of the components does not have an impact on the number of variables but can increase the number of constraints, making the problem more difficult to be solved. The complete problem for the operation optimization of the system is therefore composed by 17,378 variables (9986 continuous and 7392 binaries) and 19,800 constraints (18456 linear and 1344 quadratic). The distribution of the variables and constraint is provided in Table 2. The resulting size of the problem is relatively high, especially considering the presence of a non-negligible number of binary variables and the quadratic constraints. The model has therefore a MIQCP formulation, which has a nonlinear and nonconvex nature. The stage of development of commercial solvers of MIQCPs does not allow to solve this problem in a reasonable computational time and with an adequate accuracy. As a result, it is necessary to develop a strategy that allows to deal with the issues characterizing the problem, in order to find an alternative approach to perform the operation optimization.

It is worth to notice that the two main sources of complexity, (i.e the binary variables and the quadratic constraints) belong each one to only one of the two sub-models. In fact, the binary variables are addressed to simulate the MES, while the quadratic constraints are defined in the energy balances of the thermal network. If considered separately, the MES problem has a MILP formulation, while the model for the thermal network has a Quadratically Constrained Programming (QCP) formulation.

There are three main strategies that can be exploited to improve the execution of optimization problems: i) linearization techniques; ii) constraints relaxation; iii) decomposition techniques. Among these, decomposing the optimization can be a very interesting option, since allows to solve iteratively smaller versions of the original problem, which are simpler and faster to be managed.

In a conceptual perspective, the simulation of the thermal network is nested inside of the MES simulation. Decomposing the optimization defining the MES problem as the master problem and the thermal network problem as the slave problem could seem a natural choice. However, the presence of nonconvex constraints makes much more difficult to exploit the decomposition strategy. For this reason, the decomposition developed in the present study is based on a

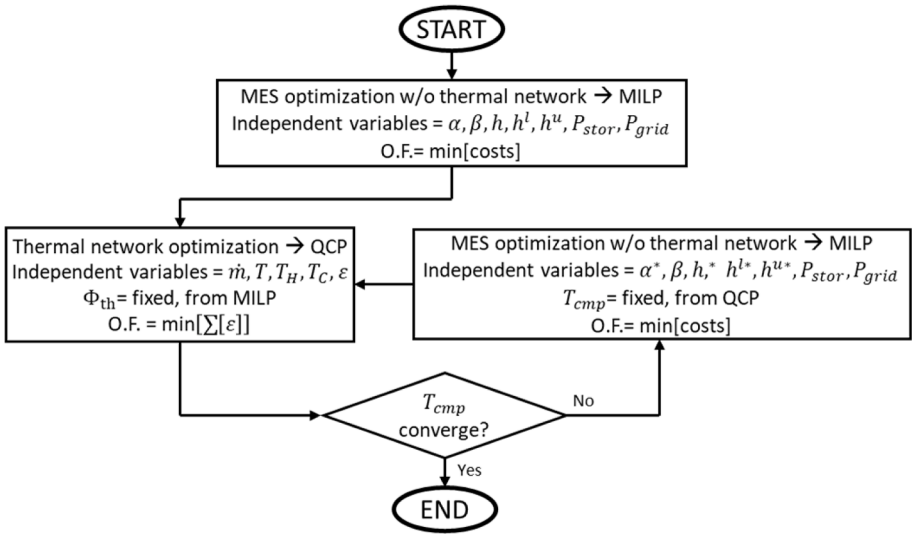

Fig. 7. Flow chart of the optimization process.

nonconventional approach. The structure of the entire optimization process is synthesized in the flowchart shown in Fig. 7.

The first step of the process consists in optimizing the MES operation without considering any variable or constraint related to the thermal network. Since the heating power produced/consumed by the thermal generators/consumers are balanced by the constraints addressed for the energy conservation, the solution obtained from this particular version of the MES optimization keeps a physical meaning. The removal of the thermal network is done with a precise purpose: obtaining a simpler problem (with a MILP formulation) that can be considered as a relaxed version of the original one. As a consequence, the independent variables addressed in this first optimization are: α, h, h^l and h^u for the linearization of the performances of the generators; P_{grid} for the powers exchanged with the external grid; P_{stor} and β for the operation of the energy storage. Any other dependent variable, such as the powers of the fuels/energy vectors, the characteristic temperatures of the thermal generators and the operating status of the components, can be computed from these independent variables. Solving this problem allows to find, among the results, the values of the T_{cmp} that minimize the operating costs in the ideally favourable case where the thermal network does not impose any kind of constraints to the MES operation.

The following step is represented by the optimization of the thermal network operation. Mass flowrates and temperatures are the parameters taken as independent variables. The thermal powers provided/consumed by the generators/users are imposed equal to the values obtained from the MES optimization. The resulting mathematical formulation is a nonconvex QCP. Despite the nonconvexity could be seen as a serious issue, the absence of integer variables and the relatively small dimensions of the problem are two crucial advantages. The aim of this step is to find the operating conditions of the network that allow to approach as much as possible the characteristic temperatures of the components found with the MES optimization. In other words, the objective is to find the mass flowrates and temperatures that allow to minimize the difference between the T_{cmp} obtained from the previous MES optimization and the T_{cmp} found optimizing the thermal network. The objective function that can be addressed is not unique since there are different ways to evaluate the error between two series of parameters. The option chosen in this study is the absolute value, as reported in Equation (33) (where k and $k-1$ are the indexes of the iteration in which the T_{cmp} is computed). It is important to notice that the errors between the T_{cmp} computed by the MILP and by the QCP will have different impacts on the operation cost, according to the importance of the component. For this reason, the absolute values are multiplied by a weight (w_c) defined for each thermal generator, obtained with a sensitivity analysis. The problem becomes therefore a minimization of maximums. Auxiliary variables (ε) and the corresponding constraints (Equation (34)) are introduced in order to rewrite the absolute values in linear form (Equation (35) and (36)).

$$OF = \sum_{c \in \mathscr{C}^{th}} \left[w_c \cdot \sum_{t \in \mathscr{T}} \left[\left| T^{t,k}_{cmp,c} - T^{t,k-1}_{cmp,c} \right| \right] \right] \tag{33}$$

$$OF = \sum_{c \in \mathscr{C}^{th}} \left[w_c \cdot \sum_{t \in \mathscr{T}} \left[\varepsilon^t_c \right] \right] \tag{34}$$

$$\varepsilon^t_c \geq T^{t,k}_{cmp,c} - T^{t,k-1}_{cmp,c} \tag{35}$$

$$\varepsilon^t_c \geq T^{t,k-1}_{cmp,c} - T^{t,k}_{cmp,c} \tag{36}$$

The successive step of the optimization process is similar to the first one. The MES operation is again optimized without taking into account the thermal network. The only difference is that all the characteristic temperatures influencing the performance of some thermal components are fixed. Their value is set equal to the respective values obtained from the previous step of the process (i.e. the optimization of the thermal network. The task required to the MES optimization is therefore reduced to find only the operating powers of the technologies, whose performances are mathematically defined by curves and not anymore by surfaces (fixing the T_{cmp} reduces the performances dependencies from two to one).

At this point, the convergence of the characteristic temperatures is evaluated. With this purpose, two parameters are defined: the maximum error among all the T_{cmp} (Equation (37)) and the maximum error among the average of the T_{cmp} for each component involved (Equation (38)). If at least one of the two errors do not satisfy the tolerance imposed, the process is repeated from the second step of the entire procedure (the optimization of the thermal network operation) until the convergence is reached.

$$\Psi^{max} = \max_{c \in \mathscr{C}^{th}; t \in \mathscr{T}} \left(\varepsilon^t_c \right) \tag{37}$$

$$\Psi^{max}_{\text{ave}} = \max_{c \in \mathscr{C}^{th}} \left(\text{avg}_{t \in \mathscr{T}} \left(\varepsilon^t_c \right) \right) \tag{38}$$

The entire model is written in the Julia language, the MILP problem is executed by Gurobi, while Ipopt is used to perform for the QCP optimization.

Table 3
Benchmarks for the convergence of the iterative process.

Iteration	O.F. MILP [€/day]	O.F. QCP [°C]	Ψ^{max} [°C]	Ψ^{max}_{ave} [°C]	Computational times [s]	
					MILP	QCP
1	102.89	255.5	16	3.7	96	59
2	103.69	9.5	2.8	0.73	128	50
3	103.74	0.02	0.03	0.002	33	70

Once that the complete structure of the model developed has been discussed, it is important to make a fundamental observation. The optimization approach presented, which is relatively similar to a fixed-point method, does not guarantee that the solution obtained at the end of the process is the global optimum. This is due to two main reasons: i) the MES and the thermal network are optimized in series and are not nested between them; ii) the result could change according to the objective function selected for the optimization of the thermal network. However, it must be reminded that the global optimum cannot be demonstrated to be reached for nonconvex problems. Making efforts in convexifying the problem could seem a good strategy for ensuring the global optimality, but the solution obtained in this case would be referred to an approximated version of the original problem, and therefore it would not delete all the issues. On the other hand, the simple structure of the process, the absence of complex mathematical tools (e.g. relaxation strategies, reformulations, etc.) adopted to execute the optimization and the computational times required (as will be demonstrated) are important and promising aspects characterizing this model. For these reasons, in authors' opinion, near-optimal solutions found with the model developed in this study can be a very useful result to attain. To further enforce the reliability of the results obtained, the outcomes will be demonstrated to be high quality solutions, "satisfyingly close" to the global optimality.

4. Results

In this section the results obtained executing the optimization procedure are presented and discussed. The values of some meaningful parameters reached during the convergence of the iterative process are reported in Table 3.

The first iteration is actually the result of the first step of the process, the MES operation optimization without the thermal network, which is executed before the iterative cycle, and the following optimization of the thermal network. The two parameters defined to evaluate the convergence state of the procedure (Ψ^{max} and Ψ^{max}_{ave}) undergo a fast decay. In fact, the entire process took three iterations, with a computational time of 8 min on a laptop with an Intel i7-1065G7 CPU and 16 GB of RAM.

As previously mentioned, this first optimization of the MES operation represents a relaxed version of the complete problem. The thermal components are free to set their operation (i.e. powers and characteristic temperatures) without taking into account the limitations imposed by the presence of the thermal network. It is not guaranteed that this relaxed global optimum can constitute a feasible operating schedule for the real case study, however, its outcome (102.89 €/day) can be taken as a useful theoretical reference. In fact, it represents an upper boundary for any feasible solution of the optimization problem. This allows to make an interesting observation regarding the quality of the near-optimal solution obtained at the end of the process. The operation costs at the final iteration are equal to 103.74 €/day, only the 0.8% higher with respect to the relaxed global optimum. This means that, since the real global optimum must be between the relaxed global optimum and the (local) optimum obtained, the solution found with this model can have, in the worst case, operation costs the 0.8% higher with respect to the global solution. The optimization process developed, despite unable to guarantee the global optimality, demonstrates to achieve high quality results (or near-optimal solutions) of a complex problem in a reasonable amount of time.

In 2 out of 3 iterations, solving the MILP problem results to be more complex with respect to the QCP problem. However, the computational times requested by the two problems are comparable between them. The MES optimization has a linear formulation, but its higher size and the presence of binary variables make it more difficult to be solved. From the second iteration, the result of the MILP from the previous iteration is provided as initial guess to the solver; in addition, once that the characteristic temperatures are fixed, the size of the MILP is reduced and the performances previously addressed with surfaces are reduced to curves. However, looking at the results of the iterative process, it is not possible to state that the solver is always able to take advantage of them. On the other hand, despite its smaller dimensions, the sources of nonconvexity and the non-trivial management of the thermal storage represent the main complexities affecting the QCP and contribute to determine its non-negligible computational time.

Regarding the other optimization outcomes, the electric and thermal powers related to all the technologies involved in the system operation are reported in Fig. 8. The diagrams are stacked area graphs, where the powers produced by the generators are reported on the positive sector of the vertical axis (intended as entering, so positive energy fluxes) and vice versa for the ones absorbed by the consumers on the negative y-axis (intended as exiting, so negative energy fluxes). Electricity generation is mainly assigned to CHP and FC, with a small (and non-adjustable) contribution from photovoltaic and wind powers. This electricity is employed to cover the load demand and supply the EHP; a remarkable excess is produced to be sold to the grid, especially when the selling price is higher. Buying the electricity from outside is an option that never takes place, while the electric storage operation is mostly devoted to the closure of the balance.

The heating demand is satisfied with only the CHP and the EHP, since the boiler and the GHP are not the most efficient and cheap alternatives.

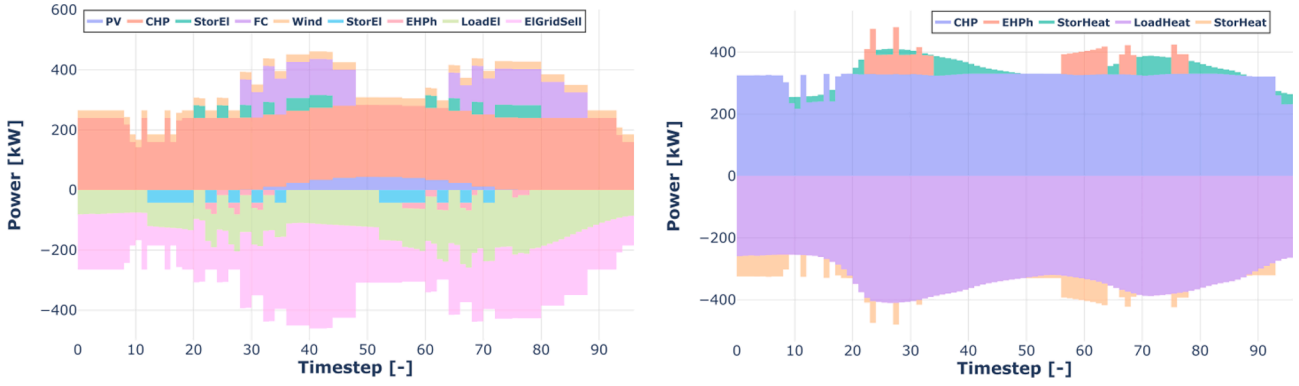

Fig. 8. Electric power (left) and heating power (right) of generators and consumers.

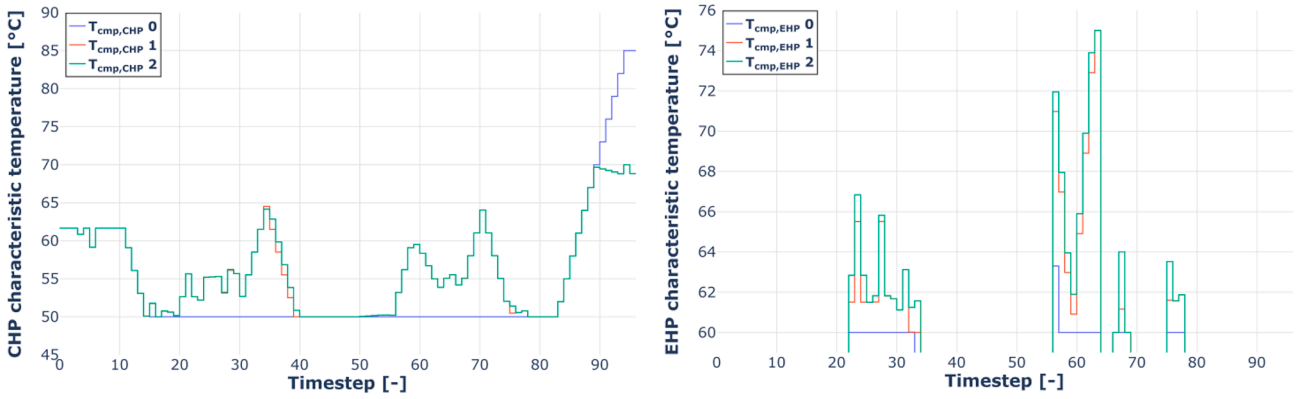

Fig. 9. Characteristic temperatures of CHP and EHP during the iterative process.

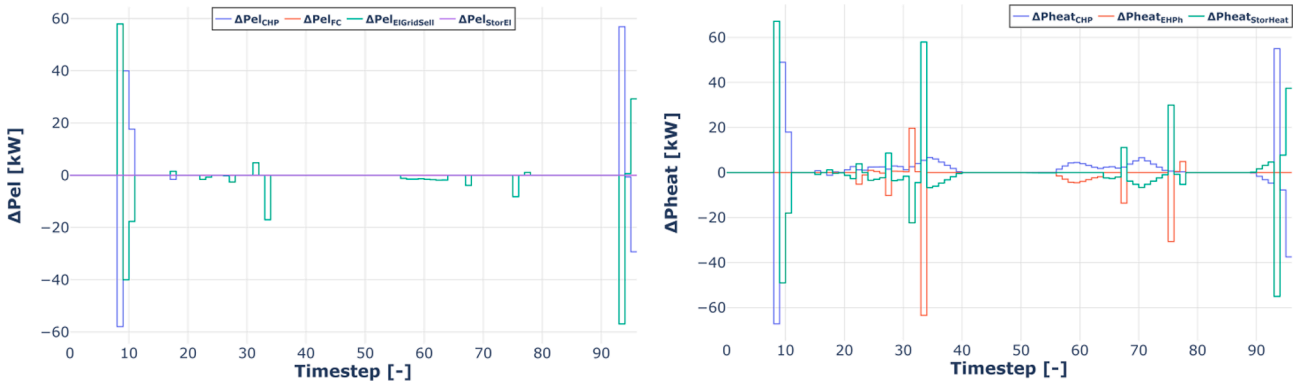

Fig. 10. Difference between first and last iteration of electrical (left) and thermal (right) fluxes.

The charging and discharging phases of the thermal storage are relatively frequent. Whenever possible, the CHP is used at its nominal load, which allows to reach the highest efficiency. The EHP and the thermal storage are used when the CHP cannot cover the thermal load on its own.

The time profile of the characteristic temperatures of the two thermal generators employed for the heating production (the CHP and the EHP) reached in the three iterations of process are reported in the two graphs of Fig. 9. Notice that when a component is not operating, the characteristic temperature is null, otherwise it assumes its real value. In both cases, the values found in the first iteration tend to be flatter, showing smaller variations during the time period analysed. This result is reasonable and can be explained considering that the MILP executed in the first iteration is the only one that does not undergo any influence from the operation of the thermal network. Consequently, the T_{cmp} reached in this step are the ones more favourable for the objective function, without taking into account the constraints that must be respected to allow the exchange of the thermal powers across the network. On the overall, the difference between the characteristic temperatures found by the MILP and the ones obtained with the QCP is minimized up to zero whenever as possible, which is favoured by the flexibility of connections in the layout of the thermal network. In addition, it can be observed that, beside the input power, the model uses the T_{cmp} as an additional parameter to regulate the operation of the component, according to the performance surface that describes its operation. However, it must be recognised that this behaviour of the characteristic temperatures is strictly related to the performance curves of the components provided as input data and cannot be taken as a universal feature.

Other interesting considerations can be made looking at the variation of the fluxes of the two main energy vectors for the most important components, reported in Fig. 10. The curves represent the difference of

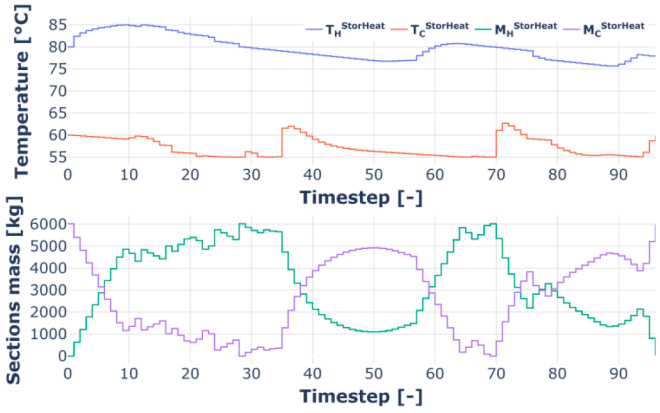

Fig. 11. Operating temperatures (up) and water masses (down) of the thermal storage.

the electrical (on the left) or thermal (on the right) powers between the values reached in the first and last iteration of the optimization process. In most of the timesteps the difference is small or null; however, in some cases the variations reach the order of magnitude of few tens of kW, which is not negligible. These adjustments are due to the variations of the characteristic temperatures, imposed in order to avoid the violations of the constraints of the thermal network. Imposing a different value of the characteristic temperature changes the performance of the component, whose operation can be modified if it results to be no more optimal in economic terms. As can be observed, in most of the cases these variations compensate each other. In fact, since the requirement of the loads is constants input parameter, the reduction in the power production of a

Table 4
Coefficients for the performance curves.

	a	b	c	d	e	P_{in}^{min}	P_{in}^{max}
CHP (el)	$-4.9 \cdot 10^{-7}$	$7.8 \cdot 10^{-4}$	0.09	0.0	0.0	358 kW	625 kW
CHP (th)	$-9.2 \cdot 10^{-8}$	$1.3 \cdot 10^{-4}$	0.48	−0.47	23.6	358 kW	625 kW
Boiler	$-6.3 \cdot 10^{-7}$	$4.1 \cdot 10^{-4}$	0.87	−0.57	28.6	110 kW	430 kW
GHP	$5.6 \cdot 10^{-5}$	$-8.0 \cdot 10^{-3}$	1.37	−0.27	19.0	45 kW	140 kW
FC	$-3.3 \cdot 10^{-7}$	$6.7 \cdot 10^{-5}$	0.40	0.0	0.0	48 kW	305 kW
EHP	$4.6 \cdot 10^{-4}$	$-1.2 \cdot 10^{-2}$	3.63	−0.34	24.0	17 kW	55 kW

Table 5
Prices of fuels and energy vectors.

	NG	LPG	H_2	El bought	El sold
Price	0.195 €/Sm^3	0.034 €/kWh	0.03 €/kWh	0.136–0.19 €/kWh	0.036–0.09 €/kWh

component is balanced with the increase of the generation of another technology. The cases in which these variations are not compensated are due to the fact that are modified peculiar elements of the MES, such as the connection with the external power grid for selling/buying electricity.

Finally, the temperatures and masses of the hot and cold water in the thermal storage are reported in Fig. 11. The model manages to integrate the storage operation (in terms of flowrates and temperatures) in the thermal network. At the first timestep, the storage is assumed to be empty (i.e. full of cold water). Then, it is charged up to its maximum for two times and at the end of the period it returns empty (as imposed by input data). The mass of hot water keeps a temperature in a range between 75 °C and 85 °C, while the cold water remains between 55 °C and 65 °C. On the overall, the storage increase the flexibility of the system and allows to achieve lower operation costs, but, at the same time, increases the dependency among the timesteps and, as a consequence, the complexity of the management of the thermal network.

5. Conclusions

In the present study, the simulation of a thermal network is included into the operation optimization of a MES in order to perform a more complete and reliable analysis. A medium-sized energy system composed by very different technologies (CHP, HoB, GHP, EHP, FC, renewable sources, electric and thermal storage, and grid connections) is taken as case study. Partial loads of components, mass flowrates and temperatures of the network are the independent variables to optimize with the purpose of minimizing the operating costs. The problem is solved iteratively with a decomposition approach and the piecewise linearization technique.

The outcome of the model is promising both for the computational time required and the numerical result. For the case study under consideration, the convergence was reached after three iterations. The production and consumption of the two main energy vectors (electricity and heating) is shown and discussed. Regarding the electricity production, the CHP and the FC are the preferred choice to cover the load and to obtain an income by selling the electricity to the external grid. Concerning the heating, the GHP and the Boiler are never switched on since the combined use of the CHP and the EHP is more efficient. The characteristic temperatures result to be an alternative to the partial loads for the regulation of the components, which have a direct and noticeable impact on the operating conditions of the thermal network. The management of the thermal storage results to be encouraging, since the model succeed in finding a suitable operation for this component, considering the most important physical phenomena characterizing the technology. On the overall, the model proved to be able to find a near-optimal solution of the problem without requiring the use of complex mathematical formulations.

Finally, as an idea for future model developments, it would be interesting to evaluate the feasibility of a study in which the simplifying hypotheses adopted for the thermal network simulation are removed. In fact, including the heat losses and the effects of thermal inertia in the model would improve the quality of the simulation of the network, increasing the applicability of the result in a real context.

CRediT authorship contribution statement

Umberto Tesio: Conceptualization, Methodology, Visualization, Writing – original draft, Writing – review & editing. **Elisa Guelpa:** Conceptualization, Methodology, Formal analysis. **Vittorio Verda:** Conceptualization, Methodology, Project administration, Funding acquisition.

Declaration of Competing Interest

The authors declare that they have no known competing financial interests or personal relationships that could have appeared to influence the work reported in this paper.

Data availability

The data that has been used is confidential.

Appendix A

Performance curves

The coefficients for the performance curve (Equation (1)) of the different technologies involved in the MES operation are arbitrary taken and reported in Table 4. In addition, the corresponding boundaries for the input powers are presented.

Concerning the two technologies exploiting renewable powers (PV and wind turbine), their power production is considered as an input data since it cannot be regulated. A peak of 43.6 kW with the generation profile of a typical winter day is assumed for the PV, while a constant production of 25 kW is considered for the wind turbine.

Energy prices

The prices of the fuels and energy vectors considered in the analysis are synthetically presented in Table 5. Only the electricity price is considered as variable during the period analysed and the extreme values are reported.

References

[1] Horowitz CA. Paris agreement. Int Leg Mater 2016;55(4):pp. https://doi.org/10.1017/s0020782900004253.
[2] IEA. Energy Efficiency 2021. Paris, 2021. [Online]. Available: https://www.iea.org/reports/energy-efficiency-2021.
[3] Speirs J, McGlade C, Slade R. Uncertainty in the availability of natural resources: fossil fuels, critical metals and biomass. Energy Policy 2015;87. https://doi.org/10.1016/j.enpol.2015.02.031.
[4] IRENA. World energy transitions outlook 1.5 C Pathway; 2021.
[5] Pfenninger S, Hawkes A, Keirstead J. Energy systems modeling for twenty-first century energy challenges. Renew Sustain Energy Rev 2014;33. https://doi.org/10.1016/j.rser.2014.02.003.
[6] Xu Y, Yan C, Liu H, Wang J, Yang Z, Jiang Y. Smart energy systems: a critical review on design and operation optimization. Sustain Cities Soc 2020;62:102369. https://doi.org/10.1016/J.SCS.2020.102369.

[7] Lund PD, Lindgren J, Mikkola J, Salpakari J. Review of energy system flexibility measures to enable high levels of variable renewable electricity. Renew Sustain Energy Rev 2015;45:785–807. https://doi.org/10.1016/j.rser.2015.01.057.

[8] Linna N, Changsen F, Wen F, Salam A. Optimal power flow of multiple energy carriers with multiple kinds of energy storage. IEEE Power Energy Soc. Gen. Meet., vol. 2016-Novem, no. 2015, 2016, doi: 10.1109/PESGM.2016.7741940.

[9] Chicco G, Mancarella P. Distributed multi-generation: a comprehensive view. Renew Sustain Energy Rev 2009;13(3):535–51. https://doi.org/10.1016/j.rser.2007.11.014.

[10] Urbanucci L. Limits and potentials of mixed integer linear programming methods for optimization of polygeneration energy systems. Energy Procedia 2018;148:1199–205. https://doi.org/10.1016/j.egypro.2018.08.021.

[11] Raheli E, Wu Q, Zhang M, Wen C. Optimal coordinated operation of integrated natural gas and electric power systems: a review of modeling and solution methods. Renew Sustain Energy Rev 2021;145:111134. https://doi.org/10.1016/j.rser.2021.111134.

[12] Pshenichnyj BN. The Linearization Method for Constrained Optimization, vol. 22. Berlin, Heidelberg: Springer, Berlin Heidelberg; 1994.

[13] Huang S, Tang W, Wu Q, Li C. Network constrained economic dispatch of integrated heat and electricity systems through mixed integer conic programming. Energy 2019;179:464–74. https://doi.org/10.1016/j.energy.2019.05.041.

[14] Kia M, Nazar MS, Sepasian MS, Heidari A, Siano P. Optimal day ahead scheduling of combined heat and power units with electrical and thermal storage considering security constraint of power system. Energy 2017;120:241–52. https://doi.org/10.1016/j.energy.2016.11.079.

[15] E. Raheli, Q. Wu, C. Wen, Feasibility verification of a MILP model by outer approximation for the optimal operation of natural gas networks, in: 2021 IEEE Madrid PowerTech, PowerTech 2021 - Conf. Proc., pp. 0–5, 2021, doi: 10.1109/PowerTech46648.2021.9494996.

[16] Lin C, Wu W, Zhang B, Sun Y. Decentralized solution for combined heat and power dispatch through benders decomposition. IEEE Trans Sustain Energy 2017;8(4):1361–72. https://doi.org/10.1109/TSTE.2017.2681108.

[17] Rahimi S, Niknam T, Fallahi F. A new approach based on benders decomposition for unit commitment problem. World Appl Sci J 2009;6(12):1665–72.

[18] E. Ikonen et al., Short term optimization of district heating network supply temperatures, ENERGYCON 2014 - IEEE Int. Energy Conf., pp. 996–1003, 2014, doi: 10.1109/ENERGYCON.2014.6850547.

[19] Morvaj B, Evins R, Carmeliet J. Optimising urban energy systems: Simultaneous system sizing, operation and district heating network layout. Energy Dec. 2016;116:619–36. https://doi.org/10.1016/J.ENERGY.2016.09.139.

[20] Costa A, Fichera A. A mixed-integer linear programming (MILP) model for the evaluation of CHP system in the context of hospital structures. Appl Therm Eng 2014;71(2):921–9. https://doi.org/10.1016/j.applthermaleng.2014.02.051.

[21] Ershadi H, Karimipour A. Present a multi-criteria modeling and optimization (energy, economic and environmental) approach of industrial combined cooling heating and power (CCHP) generation systems using the genetic algorithm, case study: a tile factory. Energy 2018;149:286–95. https://doi.org/10.1016/j.energy.2018.02.034.

[22] Bischi A, et al. A detailed MILP optimization model for combined cooling, heat and power system operation planning. Energy 2014;74:12–26. https://doi.org/10.1016/j.energy.2014.02.042.

[23] Ameri M, Besharati Z. Optimal design and operation of district heating and cooling networks with CCHP systems in a residential complex. Energy Build 2016;110:135–48. https://doi.org/10.1016/j.enbuild.2015.10.050.

[24] Abdollahi E, Wang H, Lahdelma R. An optimization method for multi-area combined heat and power production with power transmission network. Appl Energy 2016;168:248–56. https://doi.org/10.1016/j.apenergy.2016.01.067.

[25] Pan Z, Guo Q, Sun H. Feasible region method based integrated heat and electricity dispatch considering building thermal inertia. Appl Energy 2017;192:395–407. https://doi.org/10.1016/j.apenergy.2016.09.016.

[26] Zhang R, Jiang T, Li W, Li G, Chen H, Li X. Day-ahead scheduling of integrated electricity and district heating system with an aggregated model of buildings for wind power accommodation. IET Renew Power Gener 2019;13(6):982–9. https://doi.org/10.1049/iet-rpg.2018.5836.

[27] Wang Y, et al. Operation optimization of regional integrated energy system based on the modeling of electricity-thermal-natural gas network. Appl Energy 2019;vol. 251:113410. https://doi.org/10.1016/j.apenergy.2019.113410.

[28] Omu A, Choudhary R, Boies A. Distributed energy resource system optimisation using mixed integer linear programming. Energy Pol 2013;61:249–66. https://doi.org/10.1016/j.enpol.2013.05.009.

[29] L. Gurobi Optimization. Gurobi Optimizer Reference Manual. *https//www.gurobi.com/ Doc. aufgerufen am 27.10.2020*, 2020.

[30] Wächter A, Biegler LT. On the implementation of an interior-point filter line-search algorithm for large-scale nonlinear programming. Math Program 2006;106(1):pp. https://doi.org/10.1007/s10107-004-0559-y.

[31] Wang X, Bie Z, Liu F, Kou Y. Co-optimization planning of integrated electricity and district heating systems based on improved quadratic convex relaxation. Appl Energy 285(July 2020) 116439. doi: 10.1016/j.apenergy.2021.116439.

[32] Liu X, Wu J, Jenkins N, Bagdanavicius A. Combined analysis of electricity and heat networks. Appl Energy 2016;162:1238–50. https://doi.org/10.1016/j.apenergy.2015.01.102.

[33] D'Ambrosio C, Lodi A, Martello S. Piecewise linear approximation of functions of two variables in MILP models. Oper Res Lett 2010;38(1). https://doi.org/10.1016/j.orl.2009.09.005.